

PACS numbers: 42.55.Px; 42.60.Da; 42.79.Dj
DOI: 10.1070/QE2014v044n10ABEH015475

Spectral characteristics of multimode semiconductor lasers with a high-order surface diffraction grating

V.V. Zolotarev, A.Yu. Leshko, N.A. Pikhtin, A.V. Lyutetskiy, S.O. Slipchenko, K.V. Bakhvalov, Ya.V. Lubyanskiy, M.G. Rastegaeva, I.S. Tarasov

Abstract. **We have studied the spectral characteristics of multimode semiconductor lasers with high-order surface diffraction gratings based on asymmetric separate-confinement heterostructures grown by metalorganic vapour phase epitaxy (λ = 1070 nm). Experimental data demonstrate that, in the temperature range ±50 °C, the laser emission spectrum is ~5 Å in width and contains a fine structure of longitudinal and transverse modes. A high-order (m = 15) surface diffraction grating is shown to ensure a temperature stability of the lasing spectrum $d\lambda/dT$ = 0.9 Å K^{-1} in this temperature range. From analysis of the fine structure of the lasing spectrum, we have evaluated the mode spacing and, thus, experimentally determined the effective length of the Bragg diffraction grating, which was ~400 μm in our samples.**

Keywords: *semiconductor laser, distributed Bragg reflectors, higher orders of diffraction.*

1. Introduction

Owing to their unique properties, high-power semiconductor lasers have become an indispensable basic component of instruments and systems in a number of application areas. The progress of modern technologies and the advent of high-power semiconductor lasers made it possible to achieve record-high performance, including the optical power, efficiency and operational life [1, 2]. The semiconductor lasers possess, however, not only huge advantages but also some properties that limit their application fields in science and technology. One drawback of high-power semiconductor lasers with a Fabry–Perot cavity is the large width of their output spectrum and the poor temperature stability of their emission wavelength. The shape and position of the output spectrum of 'classic' semiconductor lasers with a Fabry–Perot cavity are determined primarily by the gain spectrum of their active region (quantum well). The broad spectrum is due to the multimode nature of the emission from high-power broad-stripe semiconductor lasers. The broadening of the laser output spectrum with increasing pump current is related to fundamental transport processes and carrier capture in the quantum-confined active region [2, 3]. The shift of the spectrum to longer wavelengths is caused by the heating of the active region and the associated change in its band gap.

To obtain a narrower and more temperature-stable laser output spectrum, one can use integrated components that ensure a sharp spectral dependence of the (useful) output loss. Thus, the width of a lasing spectrum and its variation with injection current and temperature will depend on the properties of a specific component. Single-mode semiconductor lasers with internal diffraction gratings have long been under development and investigation [4–6]. Since first- and second-order diffraction gratings are technologically difficult to produce in lasers with a stripe contact width of ~100 μm, an important issue was to create multimode semiconductor lasers with a long-period surface Bragg grating (order of diffraction $m > 6$) [7–10]. A significant advantage of the cavity design with a long-period surface Bragg grating over other possible approaches for narrowing and stabilising the spectrum of a semiconductor laser is the relative simplicity of the fabrication process. Since all the elements of Bragg diffraction gratings have relatively large dimensions, they are fabricated using a standard photolithographic process and reactive ion etching.

Our group's previous work was concentrated on the theoretical analysis and [7] and power performance [8] of distributed Bragg reflector (DBR) semiconductor lasers. The purpose of this work was to study the output spectra of DBR semiconductor lasers in a wide temperature range.

2. Experimental samples and main investigation techniques

Experimental samples were prepared from a laser heterostructure grown by metalorganic vapour phase epitaxy in the GaAs/AlGaAs/InGaAs solid solution system. The heterostructure had the form of an asymmetric separate-confinement double heterostructure (SCDHS): a 90-Å-thick strained InGaAs quantum well was inserted in an $Al_{20}Ga_{80}As$ waveguide layer, which was sandwiched between n- and p-emitters ($Al_{30}Ga_{70}As$ and $Al_{25}Ga_{75}As$) [11]. A surface Bragg grating was produced on the surface of the heterostructure by standard photolithographic and reactive ion etching processes (Fig. 1a). Next, using standard post-growth steps, we fabricated multimode lasers with a broad mesa stripe contact [12]. The stripe contact width (emission aperture size) was 100 μm. The diffraction grating period was 2.4 μm, which corresponded to the 15th order of diffraction in Bragg's condition for an emission wavelength of 1070 nm. A dielectric was deposited on the grating region, and an Ohmic gold–zinc contact was made on the rest of the mesa stripe. Thus, the laser chip comprised two sections: a gain (injection) section

V.V. Zolotarev, A.Yu. Leshko, N.A. Pikhtin, A.V. Lyutetskiy, S.O. Slipchenko, K.V. Bakhvalov, Ya.V. Lubyanskiy, M.G. Rastegaeva, I.S. Tarasov Ioffe Physical Technical Institute, Russian Academy of Sciences, Politekhnicheskaya ul. 26, 194021 St. Petersburg, Russia; e-mail: zolotarev.bazil@mail.ioffe.ru

Received 24 March 2014; revision received 11 April 2014
Kvantovaya Elektronika **44** (10) 907–911 (2014)
Translated by O.M. Tsarev

with an Ohmic metallic contact and a passive reflection section with a diffraction grating, through which no current flowed (Fig. 1b). The reflection section was 800 μm long, and the length of the gain section was varied from 1.5 to 3 mm. The laser chips were mounted, with their p-contact down, on a copper heat sink. The end faces of the chip (the mirrors of the Fabry–Perot cavity) were produced by cleaving.

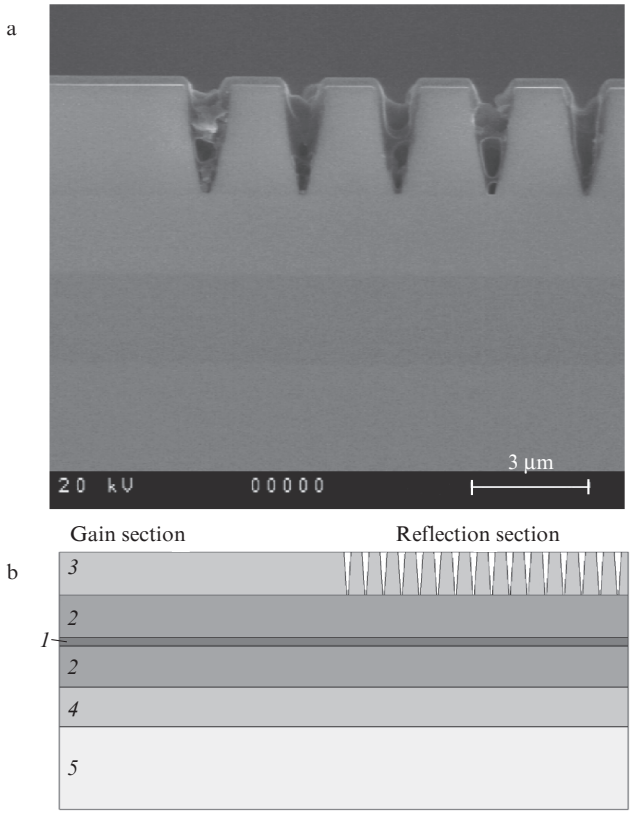

Figure 1. (a) TEM image of a surface Bragg grating on a laser heterostructure and (b) schematic of the surface DBR semiconductor laser: (*1*) active region, (*2*) waveguide, (*3*) p-emitter, (*4*) n-emitter, (*5*) substrate.

The output spectrum of the DBR semiconductor laser was measured with an Advantest Q8384 spectrum analyser. All measurements were made in cw mode. To assess the temperature effect on the laser output spectrum, the heat sink and laser were placed on a Peltier element located on a copper base with internal channels, through which water or liquid nitrogen vapour was passed. Measurements at negative temperatures (below the dew point temperature) were performed in a nitrogen vapour atmosphere to prevent frost formation on the laser chip.

3. Spectral characteristics of DBR semiconductor lasers

The output spectrum of a broad-stripe DBR semiconductor laser has a characteristic spectral width and fine inner structure (Fig. 2). The width of the output spectrum of a DBR laser is determined primarily by parameters of the Bragg diffraction grating, which include the effective refractive index contrast for electromagnetic radiation between the grating grooves and ridges and the number of lines [13]. The lower the contrast, the narrower the reflection spectrum of the DBR and, at the same time, the lower the reflectance of an individual grating line. Therefore, to reduce the width of the laser output spectrum, it is reasonable to reduce the contrast and increase the length of the DBR (increase the number of lines). The latter, however, entails an increase in internal optical loss and a decrease in differential quantum efficiency. In our experimental samples of DBR semiconductor lasers with a 15th order surface diffraction grating, the emission bandwidth was ~5 Å.

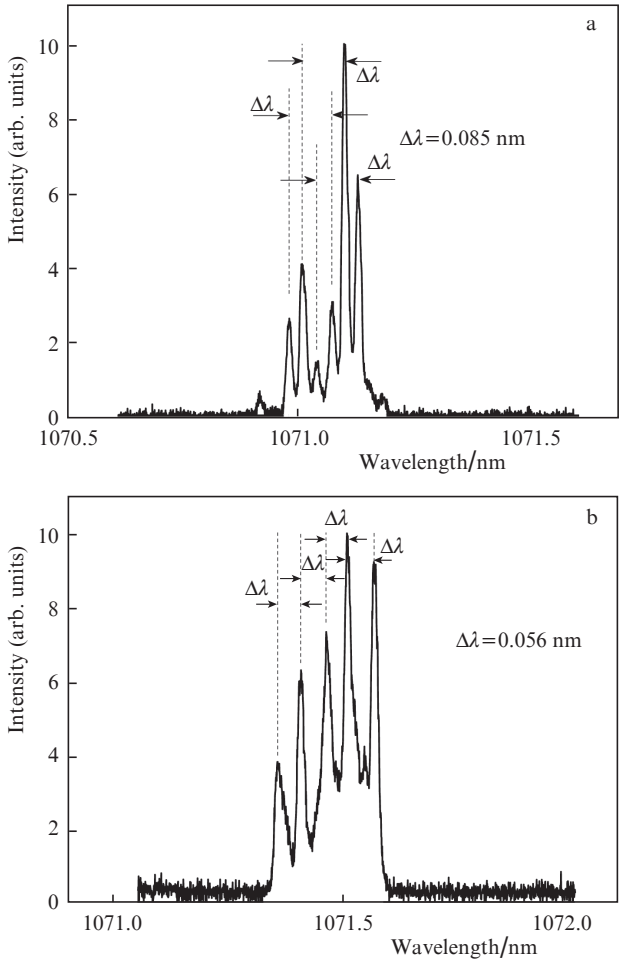

Figure 2. Output spectra of a surface DBR semiconductor laser with a reflection section 0.8 mm in length and an gain section (a) 1.6 and (b) 2.6 mm in length.

The fine structure of the output spectrum of a DBR semiconductor laser is determined by the presence of both longitudinal and transverse (lateral) cavity modes in the semiconductor laser. The spectrum has a dominant mode, whose intensity exceeds that of the other cavity modes (Fig. 2). The large number of longitudinal modes in the output spectrum of the DBR semiconductor laser is due to the long cavity length. The requirement to increase the cavity length of the DBR laser is related to the fact that it is based on a separate-confinement heterostructure with a low internal loss, and increasing the cavity length is necessary for reaching an appropriate gain in the heterostructure [14]. The presence of transverse modes in the plane normal to the layers of the heterostructure is determined by the parameters of the waveguide in the

SCDHS. In our case, the laser operates in a single (fundamental) transverse mode. This is supported by far-field measurements along the normal to the epilayers of the heterostructure. The large number of lateral modes in the plane parallel to the epilayers of the laser heterostructure can be accounted for by the laser stripe contact width (100 μm) considerably exceeding the emission wavelength.

Thus, as pointed out above, the emission bandwidth of the DBR laser can be reduced by optimising parameters of the Bragg diffraction grating. To this end, one more parameter (along with the grating length and effective refractive index contrast) should be taken into account: effective grating length. Since the phase change of an electromagnetic wave near a reflection maximum can be thought to be linear, let us represent a DBR by a discrete mirror located one effective length from the origin of the grating [15]. Thus, the spectral spacing between neighbouring longitudinal modes is determined by the sum of the length of the gain section and the effective grating length:

$$\Delta\lambda = \frac{\lambda^2}{2nL_{\Delta\lambda}}, \tag{1}$$

$$L_{\text{eff}} = L_{\Delta\lambda} - L_{\text{gs}} = \frac{\lambda^2}{2n\Delta\lambda} - L_{\text{gs}}, \tag{2}$$

where $\Delta\lambda$ is the spectral spacing between neighbouring longitudinal modes; λ is the laser wavelength; n is the effective refractive index of the medium; L_{gs} is the length of the gain section; $L_{\Delta\lambda}$ is the calculated total cavity length; and L_{eff} is the effective length of the Bragg grating.

We experimentally determined the effective length of the diffraction grating by measuring the mode spacing in semiconductor lasers having different lengths of the gain section. In our experimental samples, the standard length of the reflection section was 0.8 mm, and the length of the gain section was 1.6, 2.2 or 2.6 mm. Figure 2 shows typical output spectra of the experimental samples of DBR semiconductor lasers. Table 1 lists the mode spacings, calculated cavity lengths, gain section lengths and effective DBR lengths. For all the types of DBR semiconductor lasers, L_{eff} is ~400 μm. It is worth pointing out that the large number of lateral modes (especially in the DBR lasers with short cavity lengths) made it difficult to determine the mode spacing, because we failed to find a set of equidistant longitudinal modes in some of the lasing spectra (Fig. 2a).

Table 1. Parameters of the DBR lasers.

Length of the gain section/mm	Mode spacing/nm	Calculated cavity length/mm	Effective Bragg grating length/mm
1.648	0.085	2.054	0.406
2.240	0.065	2.631	0.391
2.600	0.056	3.012	0.412

4. Temperature-dependent spectral characteristics of DBR semiconductor lasers

One drawback of a stripe semiconductor laser with a Fabry–Perot cavity is that a pump current and heating of the crystal of the laser diode shift its output spectrum. The main reason for this is that its gain spectrum varies with temperature. The band gap of III–V solid solutions decreases with increasing temperature and, as a consequence, their emission spectrum shifts to longer wavelengths at a rate of 3 to 5 Å K^{-1}, depending on the semiconductor solid solution system.

The spectra of the other parameters (external and internal optical losses) in the expression for the lasing threshold exhibit a very small or no temperature dependence:

$$g = \alpha_{\text{int}} + \alpha_{\text{out}}, \tag{3}$$

where g is the modal gain; α_{int} is the internal optical loss; and α_{out} is the (useful) output loss.

The output spectrum of DBR semiconductor lasers varies rather little with temperature. Its variation is determined by the temperature dependence of the reflection spectrum of the Bragg diffraction grating. Bragg's condition for the emission wavelength of the DBR laser has the form

$$\lambda = \frac{2n\Lambda}{m}. \tag{4}$$

This condition includes the effective refractive index n of the waveguide layer in the laser heterostructure and the diffraction grating period Λ, which are temperature-dependent. The temperature coefficient of the refractive index of $Al_{30}Ga_{70}As$ is $\partial n/\partial T = 2.5\times10^{-4}$ K^{-1} [16]. The linear thermal expansion coefficient of $Al_xGa_{1-x}As$ solid solutions is $\Lambda^{-1}\partial\Lambda/\partial T = (5.73 - 0.53x)\times10^{-6}$ K^{-1} [17, 18]. Thus, we can estimate the temperature-induced shift of the reflection spectrum of the distributed Bragg reflector on the surface of the multimode semiconductor laser:

$$\frac{d\lambda}{dT} = \frac{\lambda}{n}\left(\frac{\partial n}{\partial T} + n\Lambda^{-1}\frac{\partial\Lambda}{\partial T}\right) \approx 0.86 \text{ Å K}^{-1}.$$

Figure 3 illustrates the temperature effect on the output spectrum of the DBR semiconductor laser. With increasing temperature, the spectrum shifts to longer wavelengths. The lasing bandwidth is within 5 Å throughout the temperature range studied. Figure 4 shows the temperature-dependent position of the main maximum in the output spectrum of the

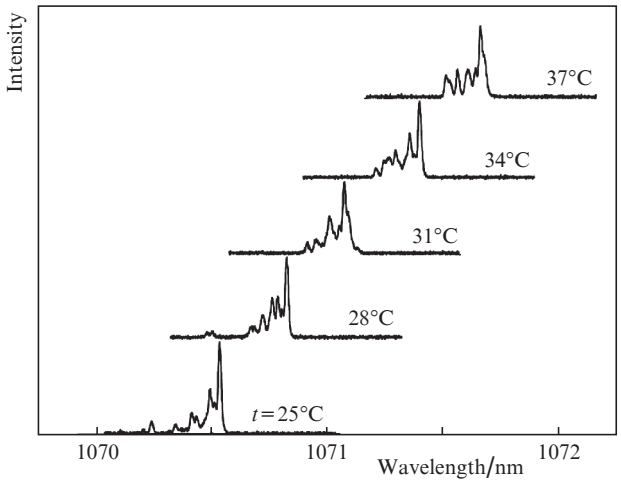

Figure 3. Temperature effect on the output spectrum of the surface DBR semiconductor laser.

DBR laser in the temperature range 25–40 °C. The maximum shifts at a rate of ~1 Å K^{-1}. When the frequency of the eigenmode reaches the edge of the reflection spectrum of the DBR, a jump occurs and another longitudinal mode becomes the main maximum. In some instances, we observe competition between several longitudinal modes. This occurs especially often in lasers with a small cavity length.

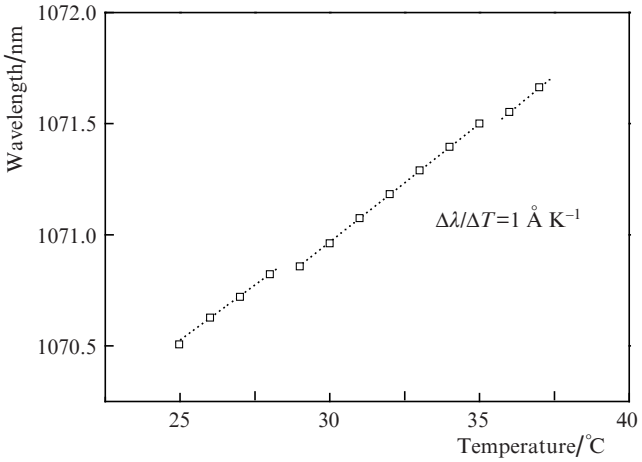

Figure 4. Temperature effect on the position of the main maximum in the output spectrum of the surface DBR semiconductor laser. The open squares represent the experimental data and the dashed lines represent fitting results.

Figure 5 shows the temperature dependence of the long-wavelength edge of the laser output spectrum. The measurements were made in the temperature range ±60 °C. Lasing was observed in the temperature range ±50 °C. Raising or lowering the temperature beyond this range resulted in the termination of lasing. The reason for this is that, with increasing temperature, the gain spectrum of the active region and the reflection spectrum of the DBR shift at different rates. When the critical temperatures are reached, the gain decreases to the point where lasing ceases. The dependence is linear with a slope $d\lambda/dT = 0.9$ Å K^{-1}, which agrees reasonably well with the above calculation results and is of the same order as an experimentally determined value reported previously [19].

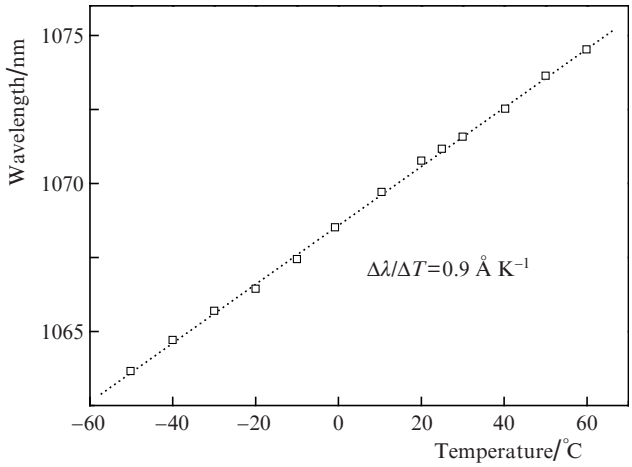

Figure 5. Temperature dependence of the long-wavelength edge of the output spectrum of the surface DBR semiconductor laser. The open squares represent the experimental data and the dashed line represents fitting results.

Our experimental samples were prepared so that the maximum of the gain spectrum of the active region coincided with the reflection spectrum of the DBR at room temperature and low injection currents. At an excitation level of ~$6I_{th}$ (where I_{th} is the threshold current), lasing ceased at temperatures below −50 °C and above +50 °C. Thus, for this type of laser heterostructure, the temperature interval in which a DBR lasers operates is ~100 °C.

5. Conclusions

The integration of multimode separate-confinement semiconductor lasers with ultralow internal optical losses [2, 14] and surface Bragg diffraction gratings of high orders (m = 15 in this study) [7–10, 19] has made it possible to reduce the lasing bandwidth to 5 Å and the temperature coefficient of the laser wavelength to 0.9 Å K^{-1}. The temperature interval in which the gain spectrum of the semiconductor laser and the reflection spectrum of the DBR coincide to the extent that threshold conditions are fulfilled is ±50 °C. Since multimode semiconductor lasers have a large set of longitudinal and transverse (lateral) modes, their output spectrum has a fine internal mode structure, which cannot be eliminated. At the same time, adjusting the contrast and effective length of the diffraction grating and reducing the internal optical loss in the separate-confinement laser heterostructure, one can significantly optimise the characteristics of the DBR and reduce the emission bandwidth of the DBR semiconductor laser.

Acknowledgements. This work was supported by the Physical Sciences Division of the Russian Academy of Sciences (Programme No. III-7).

References

1. Crump P., Erbert G., Wenzel H., Frevert C., Schultz C.M., Hasler K.-H., Staske R., Sumpf B., Maaβdorf A., Bugge F., Knigge S., Tränkle G. *IEEE J. Sel. Top. Quantum Electron.*, **19** (4), 1501211 (2013).
2. Pikhtin N.A., Slipchenko S.O., Sokolova Z.N., Stankevich A.L., Vinokurov D.A., Tarasov I.S., Alferov Zh.I. *Electron. Lett.*, **40** (22), 1413 (2004).
3. Sokolova Z.N., Tarasov I.S., Asryan L.V. *Fiz. Tekh. Poluprovodn.*, **45** (11), 1553 (2011).
4. Hofstetter D., Zappe H.P., Epler J.E., Sochtig J. *Electron. Lett.*, **30** (22), 1858 (1994).
5. Roh S.D., Hughes J.S., Lammert R.M., Osowski M.L., Beernink K.J., Papen G.C., Coleman J.J. *IEEE Photonics Technol. Lett.*, **9** (3), 258 (1997)
6. Nguyen T.-P., Schiemangk M., Spieβberger S., Wenzel H., Wicht A., Peters A., Erbert G., Tränkle G. *Appl. Phys. B*, **108** (4), 767 (2012).
7. Vasil'eva V.V., Vinokurov D.A., Zolotarev V.V., Leshko A.Yu., Petrunov A.N., Pikhtin N.A., Rastegaeva M.G., Sokolova Z.N., Shashkin I.S., Tarasov I.S. *Fiz. Tekh. Poluprovodn.*, **46** (2), 252 (2012).
8. Zolotarev V.V., Leshko A.Yu., Lyutetskiy A.V., Nikolaev D.N., Pikhtin N.A., Podoskin A.A., Slipchenko S.O., Sokolova Z.N., Shamakhov V.V., Arsent'ev I.N., Vavilova I.S., Bakhvalov K.V., Tarasov I.S. *Fiz. Tekh. Poluprovodn.*, **47** (1), 124 (2013).
9. Fricke J., Wenzel H., Matalla M., Klehr A., Erbert G. *Semicond. Sci. Technol.*, **20** (11), 1149 (2005).
10. Fricke J., John W., Klehr A., Ressel P., Weixelbaum L., Wenzel H., Erbert G. *Semicond. Sci. Technol.*, **27** (5), 055009 (2012).

11. Slipchenko S.O., Podoskin A.A., Vinokurov D.A., Bondarev A.D., Kapitonov V.A., Pikhtin N.A., Kop'ev P.S., Tarasov I.S. *Fiz. Tekh. Poluprovodn*., **47** (8), 1082 (2013).
12. Vinokurov D.A., Zorina S.A., Kapitonov V.A., Murashova A.V., Nikolaev D.N., Stankevich A.L., Khomylev M.A., Shamakhov V.V., Leshko A.Yu., Lyutetskiy A.V., Nalet T.A., Pikhtin N.A., Slipchenko S.O., Sokolova Z.N., Fetisova N.V., Tarasov I.S. *Fiz. Tekh. Poluprovodn*., **39** (3), 388 (2005).
13. Agrawal G.P., Dutta N.K. S*emiconductor Lasers* (New York: New York Press, 1993).
14. Slipchenko S.O., Vinokurov D.A., Pikhtin N.A., Sokolova Z.N., Stankevich A.L., Tarasov I.S., Alferov Zh.I. *Fiz. Tekh. Poluprovodn*., **38** (12), 1477 (2004).
15. Coldren L.A., Corzine S.W. *Diode Lasers, Photonic Integrated Circuits* (New York: John Wiley & Sons Inc., 1995).
16. Gehrsitz S., Reinhart F.K., Gourgon C., Herres N., Vonlanthen A., Sigg H. *J. Appl. Phys*., **87** (11), 7825 (2000).
17. Novikova S.I. *Teplovoe rasshirenie tverdykh tel* (Thermal Expansion of Solids) (Moscow: Nauka, 1974).
18. Adachi S. *J. Appl. Phys*., **58** (3), R1 (1985).
19. Fricke J., Bugge F., Ginolas A., John W., Klehr A., Matalla M., Ressel P., Wenzel H., Erbert G. *IEEE Photonics Technol. Lett*., **22** (5), 284 (2010).